Impedance Properties and Radiation Efficiency of Electrically Small Double and Triple Split-Ring Antennas for UHF RFID Applications

Milan Polivka, *Member, IEEE,* Alois Holub, Michal Vyhnalik, Milan Svanda

***Abstract*—The present paper is targeted at investigation of electrically small planar antennas, formed by double- and triple-split rings that are intended to serve as tag antennas operated within the European UHF RFID band. An extensive systematic study of possible geometrical configurations demonstrates the range of their achievable input impedances (complex conjugate to typical UHF RFID integrated circuits) in case that both structures electrically decrease below the limit for electrically small antennas, i.e. *ka* < 0.5. The advantage of triple split ring version over the standard double split ring one consists in reduction in its electrical size and concurrent maintenance of the required range of input impedances and high radiation efficiency. Samples of both structures were manufactured, measured and their electrical properties critically compared.**

***Index Terms*—Electrically small antenna, loop antenna, radio frequency identification, split ring antenna, tag antenna.**

I. Introduction

RADIO FREQUENCY Identification (RFID) systems have been increasingly gaining ground in massive utilization in many industrial, commercial, entertainment and other branches. Over the years, the UHF RFID systems have expanded from identification of bulky object (i.e. pallets) to smaller ones (boxes on the pallets) and even proceeded to the level of small items in boxes. The number of items in the range of reader increases rapidly and identified objects are getting smaller. This development makes great demands on small tag antennas with high radiation efficiency, which strongly affects the read range.

Performance properties of electrically small antennas (ESA) [1] are determined by fundamental rule that is frequently called the *Chu limit* [2], [3], which limit their minimum quality factor *Q* that is inversely proportional to the bandwidth-efficiency product $BW\eta$. This is given by the expression $Q_{min} = 1/k^3a^3 + 1/ka$, where *ka* stands for the electrical diameter of the sphere circumscribing the largest antenna dimension. In case of non-spherical non-magnetic ESA, the principal bound taking into account the antenna shape [4], [5] provides more appropriate values for Q_{min}. These are computed using the relation: $Q_{min} = 1.5/(ka)^3/\gamma_1^{norm}$, where γ_1^{norm} is the normalized eigenvalue of electro-static polarizability. The value of $\gamma_1^{norm} \leq 1$ implies larger $Q_{\min}$ and consequently lower $BW_{\max}$ for non-spherical geometries. Although the fundamental limitations cannot be broken, the performance improvement of RFID tag antennas as ESAs still represents an attractive topic of antenna research.

Apart from miniaturisation, UHF RFID tag antennas for remote identification require a complex input impedance conjugate to the impedance of integrated circuit used (IC or simply a chip), which is generally capacitive [6]. The typical required ranges of real R_{ant} and imaginary X_{ant} parts of antenna input impedance range from 15 to 50 Ω and from 100 to 400 Ω, respectively. Methods used to achieve the required inductive input impedance typically comprise the use of folded dipole [7], multiple-arm folded dipole operated above the half-wavelength resonance [8], inductive coupled dipole spiral antenna [9] or coupling the dipole to a small loop [10]. Loop-type antennas represent another applicable type of antennas. Basically, when made electrically small, they exhibit the required inductive input impedance. Antennas based on split rings (SR) coupled with a small inner feeding loop were used in [11, 12]. The half set-up arrangement over the ground plane is presented in [13, 14]. Multi-SR antennas were also investigated by authors of the present paper in [15, 16].

In this paper, we investigate tag antennas composed of two and three concentric split rings (2-SR and 3-SR), where the inner ring is fed by RFID chip; see Fig. 1. An extensive systematic study of their achievable complex input impedance and radiation efficiency ranges for different electrical sizes is performed. The advantages of the proposed 3-SR over the standard 2-SR tag antenna for the given electrical size *ka* is illustratively demonstrated using the Smith chart. It is marked as the range of achievable input impedances together with the value of radiation efficiency, whereas the area delimited by a curved trapezoid denotes a typical range of required input impedance; see Fig. 2b. The selected 2-SR and 3-SR tag antennas matched to the particular impedance of RFID chip are fabricated and a detailed measurement of their impedance bandwidths and radiation properties is performed.

Manuscript received in September, 2012; accepted February 2013. This work has been partly supported by projects of Czech Science Foundation 102/08/1282, P102/12/P863, projects of Czech Technical University in Prague SGS10/271/OHK3/3T/13, COST projects IC 1102 VISTA, and LD 12055 AMTAS.

The authors are with the Department of Electromagnetic Field, Czech Technical University in Prague, Technicka 2, 166 27 Prague, Czech Republic (e-mail of the corresponding author: polivka@fel.cvut.cz).

Digital Object Identifier inserted by IEEE.

II. Achievable Input Impedance and Radiation Efficiency of Electrically Small Double and Triple Split-Ring Antennas

The application of 2-SR antenna, consisting of a small internal loop (fed by a chip) coupled to an outer SR, represents an effective way how to design a small tag antenna. The outer split ring is actually a curved dipole operating close to the half-wavelength resonance of the circumference $C \sim \lambda/2$ with corresponding radius $a = C/2\pi \sim \lambda/12$. It just meets the definition limit $ka = 0.5$ for electrically small antennas [1], where $k = 2\pi/\lambda$ is the free space wave number and a denote radius of the smallest sphere enclosing the antenna. If such 2-SR tag antenna is miniaturized below the given limit $ka = 0.5$, the range of its achievable complex input impedance is limited (see the text below). To explore the influence of an additional SR on the extension of achievable input impedance range, we made a performance comparison study of extensive set of 2-SR and 3-SR tag antennas. All results were achieved by EM simulator IE3D based on a method of moments.

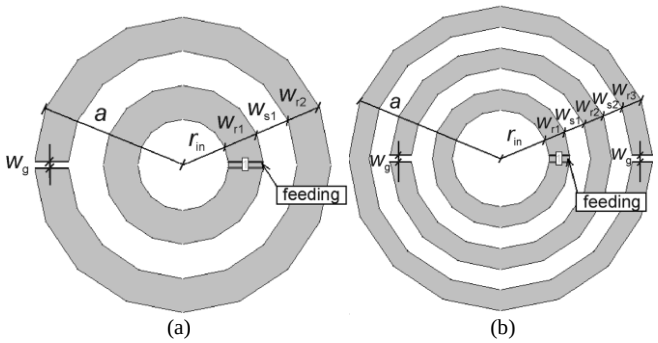

Fig. 1. Sketch of 2-SR and 3-SR antenna geometry. In both cases, the inner SR is supposed to be fed by RFID chip.

To exhibit performance of the geometry, the structures are investigated without supporting dielectric substrate at the frequency of 869 MHz that is chosen to fit into the European UHF RFID band. The 2-SR antenna geometry (Fig. 1a) has four degrees of freedom (parameters) for fixed outer dimension a that defines a particular electrical size ka: inner radius r_{in} of the inner ring, strip width W_{r1} of the inner ring, width W_{s1} of the slot between the rings, strip width W_{r2} of the outer ring, and a gap width W_g of the outer ring. The 3-SR antenna has additional two degrees of freedom: the width W_{s2} of the slot between the middle and outer rings, and the strip width W_{r3} of the outer ring; see Fig. 1b. In case of 2-SR version, the outer diameter is expressed as $a = r_{in} + W_{r1} + W_{s1} + W_{r2}$. In case of 3-SR version, this equals $a = r_{in} + W_{r1} + W_{s1} + W_{r2} + W_{s2} + W_{r3}$. The radius of internal ring is limited to $r_{in} \geq 3$ mm. The maximum gap W_g of outer ring has been chosen to amount to 2 mm. In case of 3-SR version, both gaps are chosen to be identical, i.e. $W_{g1} = W_{g2} = W_g$.

To explore the range of achievable input impedances of both double and triple SR antennas, we systematically investigate performance properties of all possible geometries for the predefined set of external dimensions within the limit $0.25 \leq ka \leq 0.5$ with a step of 0.8 mm for all above-defined dimensions. In other words, it concerns the variations of values r_{in}, W_{ri}, W_{si}, W_g while $i \in \{1, 2, 3\}$, which were generated by the Matlab script and consequently automatically analysed by IE3D simulator. By virtue of inclusion of structures with thinner strips or slots between them, the said numerous simulations were extended by all geometries where each parameter is changed with a smaller step (0.4 mm).

The results of a large number of simulations are presented as a "cloud" of input impedances in Smith chart for decreasing electrical size; see Fig. 2. Individual tag antenna geometries are indicated by dots, while the hue of the dot determines the level of radiation efficiency: black denotes $\eta_r > 80$ %, grey represents $80\ \% > \eta_r > 65\ \%$ and white indicates $65\ \% > \eta_r > 50\ \%$.

Geometries with radiation efficiency lower than 50% are not included in the Smith chart, because their introduction would reduce transparency of the pictures.

We found the smallest electrical size $ka = 0.47$ ($a = 26$ mm @869 MHz), which the input impedance of a standard 2-SR antenna is completely filled in the required input impedance area for (defined by a curved trapezoid); see Fig. 2a. Further miniaturization shifts the impedance 'cloud' toward the rim of Smith chart and for $ka < 0.4$ (see Fig. 2b) the 'cloud' moves completely out of the requested area. The smaller the antenna dimensions the more significant the reduction in the radiation efficiency. Even for $ka = 0.4$ ($a = 22$ mm @869 MHz), there are a few structures showing $\eta_r > 80$ %. The maximum simulated radiating efficiency reached $\eta_r = 90.7$ %.

Given these results, it can be argued that the major issue of the small 2-SR antenna consists in the impossibility to cover the whole required impedance area. Therefore, the 2-SR tag antenna that is smaller than $ka = 0.4$ is unsuitable for matching to typical UHF RFID chips.

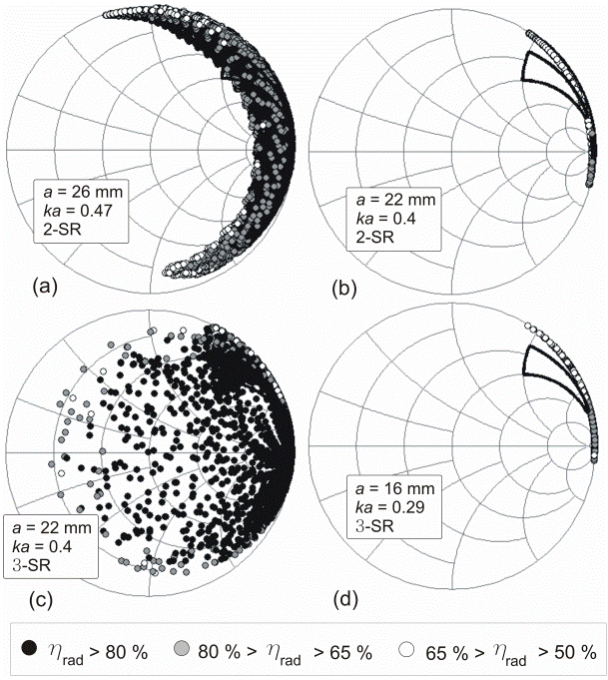

Fig. 2. Achievable range of complex input impedances for investigated sets of tag antennas: (a) 2-SR, $ka = 0.47$, (b) 2-SR, $ka = 0.40$, (c) 3-SR, $ka = 0.40$, (d) 3-SR, $ka = 0.29$. Typical range of required tag input impedance ($R_{tag} = 15 \div 50\ \Omega$ and $X_{tag} = 100 \div 400\ \Omega$) is represented by area delimited by curved trapezoid; see Fig. 2b and 2d. Black, grey, and white dots indicate respective ranges of radiation efficiency.

For further possible miniaturization of the SR-type tag antenna, we implemented and investigated the version involving three split rings (3-SR). Although in this case, the number of possible geometries increases rapidly, the setting of parameter sweep (i.e. the step, including dimensions of 0.4 mm and the low limit for r_{in}) was preserved. The additional SR significantly affects the achievable range of input impedances. Although for ka = 0.4, the input impedance of 2-SR structure remains at the rim of Smith chart (Fig. 2b), input impedances of 3-SR antenna of the same size completely fills in, again, the required impedance area (Fig. 2c). The additional SR thus enables a further miniaturization of this type of antenna.

For both 2-SR and 3-SR structures, the number of bullet marks in impedance 'cloud' is dropping provided that the size ka decreases. This phenomenon originates from the fall of radiation efficiency below $\eta_r = 50\%$ (these structures are excluded from the chart). The miniaturization limit of 3-SR antennas found by systematic investigation of the above specified range of geometries is about ka = 0.29 (a = 16 mm @869 MHz), which means that the impedance 'cloud' shifted the rim of Smith chart and it is impossible to cover the whole required impedance range with the efficiency $\eta_r > 50$ %. Such findings are helpful for proper selection of the tag antenna geometry when small size and particular complex input impedance have to be concurrently achieved.

The current density distribution of small 2-SR and 3-SR antennas are depicted in Fig. 3 (a, b). The currents on the outer split ring(s) obviously flow in the direction concurrent with the inner loop so that the respective radiation patterns correspond to the radiation of a small loop with constant current distribution along its perimeter, providing a nearly omnidirectional pattern in the plane of antenna motifs; see Fig. 3 (c, d).

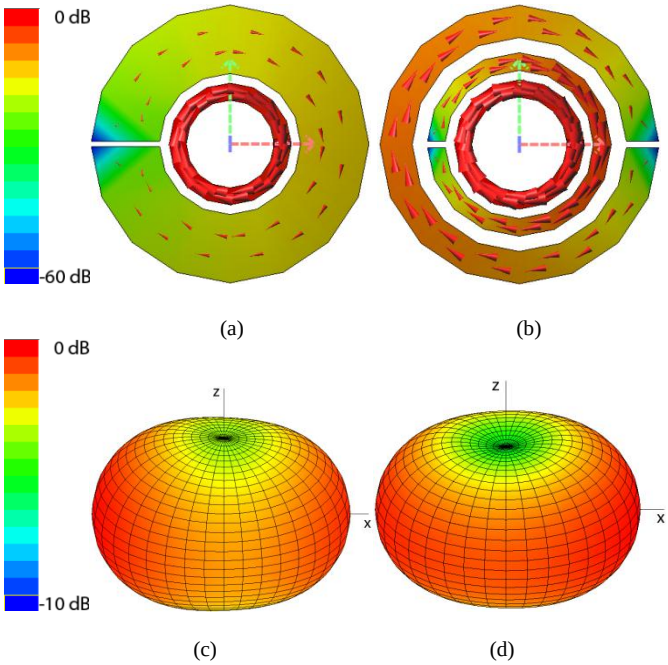

Fig. 3. Simulated vector current density distribution (a, b), and respective radiation patterns for total electric field (c, d) of 2-SR and 3-SR antennas at f = 869 MHz.

III. Parameters of Fabricated Split-Ring Antennas

In order to verify real impedance and radiation parameters of investigated antennas, two samples of 2-SR and 3-SRs UHF tag antennas were manufactured (see Fig. 4) on a thin Taconic TLP-3 substrate of the height h = 0.127 mm (its relative permittivity equals ε_r = 2.33 and loss tangent is tgδ = 0.0009 @10 GHz), both closely matched to the chip input impedance Z_{chip} = 16 – j350 Ω. The measurement of tag antenna input impedance was performed in the half-loop arrangement with the ground plane size of 145×145 mm; i.e. 0.42×0.42 λ@869 MHz.

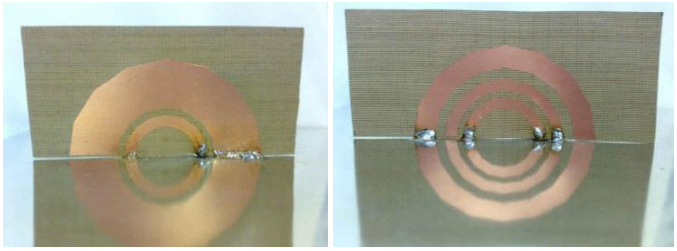

Fig. 4. Photograph of fabricated 2-SR and 3-SR tag antennas in half-loop arrangement with feeding port placed at the inner ring. Ground plane size equals 145×145 mm; i.e. 0.42×0.42 λ at frequency 869 MHz.

The measured input impedance has to be subsequently compared with the half of chip impedance; i.e. $Z_{chip}/2$ = 8 – j175 Ω; which stands for the analogy between dipole and monopole arrangements.
Their geometrical, simulated and measured parameters are depicted in Tab. 1 and 2, respectively.

TABLE I
GEOMETRICAL PARAMETERS OF 2-SR AND 3-SR TAG ANTENNAS DESIGNED FOR RFID CHIP WITH IMPEDANCE Z_{CHIP} = 16 - j350 Ω

Tag	a (mm)	ka (-)	r_{in} (mm)	W_p (mm)	W_m (mm)	W_{p2} (mm)	W_{m2} (mm)	W_{p3} (mm)
2-SR	26	0.47	8.2	3.2	1.8	12.8	-	-
3-SR	22	0.4	7.5	2.7	2.8	5.1	1.5	2.4

TABLE II
SIMULATED (FULL LOOP) AND MEASURED (HALF-LOOP) ELECTRICAL PARAMETERS OF 2-SR AND 3-SR TAG ANTENNAS AT f = 869 MHz

Tag	$R_{sim}/2$ (Ω)	$X_{sim}/2$ (Ω)	R_{meas} (Ω)	X_{meas} (Ω)	BW_{sim} (%)	BW_{meas} (%)	$\eta_{r,\,sim}$ (%)	$\eta_{r,\,meas}$ (%)	D_{sim} (dBi)
2-SR	8.2	174.4	6.6	178.9	3.1	2.5	92.1	88.9	1.7
3-SR	8.3	174.2	19.8	193.6	1.8	2.0	89.9	88.8	1.7

The radiation efficiency was measured with the help of Wheeler cap method [17], where the cap size amounted to 120×120×120 mm. The fractional half power impedance bandwidth was determined from the curve of power transmission coefficient (taking into account half-loop arrangement), evaluated from the measured complex antenna input impedance; see (1) and Fig. 5.

$$\tau = 1 - |\Gamma|^2 = \frac{4R_{ant}R_{chip}}{(R_{ant}+R_{chip})^2+(X_{ant}+X_{chip})^2} \quad (1)$$

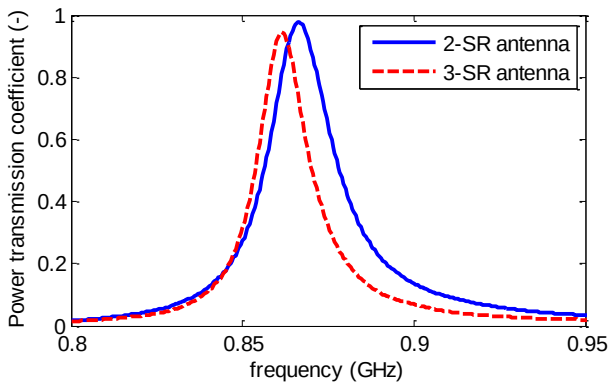

Fig. 5. Power transmission coefficient of 2-SR and 3-SR tag antennas, evaluated from measured input antenna impedance on the basis of (1).

Apart from difference in their electrical sizes, a slightly narrower impedance bandwidth of 3-SR version represents the only remarkable electrical difference between 2-SR and 3-SR antennas.

IV. Conclusion

Although the double-split ring antenna with electrical size of $ka \sim 0.5$ meets requirement of electrically small antenna, its practical utilization as UHF RFID tag antenna is limited only to structures with electrical size of approx. $ka \geq 0.47$ ($a \sim \lambda/13$). Further miniaturization significantly decreases the range of achievable complex input impedances that are complex conjugates to typical RFID chip impedances (R_{chip} ranging from 15 to 50 Ω and X_{chip} from -100 to -400 Ω).

As it has been observed from the systematic EM simulation of the large set of antenna configurations showing the electrical radius within the range $0.25 \leq ka \leq 0.5$, the implementation of additional third split ring enables a further reduction of the outer electrical size as far as to approx. $ka = 0.29$ ($a = \lambda/21$). At the same time, it is possible to maintain the required range of input impedances above this size as well as the sufficiently high radiation efficiency ($\eta_r > 50\%$). This finding might be helpful for selection of proper structure within split-ring type antenna structures, provided that the miniaturization is demanded as a key feature.

Although the impedance bandwidth is quite narrow, the investigated tag antennas sufficiently cover the European UHF RFID band of 865-869 MHz.

References

[1] H. A. Wheeler, "Fundamental limitations of small antennas," *Proc. IEEE*, vol. 35, no. 12, pp. 1479-1484, Dec. 1947.

[2] J. Chu, "Physical limitations of omni-directional antennas," *J. Appl. Phys*, vol. 10, pp. 1163-1175, Dec. 1948.

[3] J. S. McLean, "A re-examination of the fundamental limits on the radiation Q of electrically small antennas," *IEEE Trans. Antennas Propagat.*, vol. 44, no. 5, pp. 672-676, May 1996.

[4] M. Gustafsson, C. Sohl, and G. Kristensson, "Physical limitations on antennas of arbitrary shape," *Proc. R. Soc. A*, vol. 463, pp. 2589–2607, 2007.

[5] M. Gustaffson, K. Sohl, G. Kristensson, "Illustrations of new physical bounds on linearly polarized antennas," *IEEE Trans. Antennas Propagat.*, vol. 57, no. 5, pp. 1319-1327, May 2009.

[6] K. Finkenzeller, K., *RFID Handbook: Fundamentals and Applications in Contactless Smart Cards and Identification*, 2nd edition, John Wiley & Sons, Chichester, 2003.

[7] X. Qing and N. Yang, "A folded dipole antenna for RFID," In *Proc. IEEE Antennas Propagat. Soc. Int. Symp.*, Monterey, CA, vol.1, pp. 97–100, 2004.

[8] M. Svanda and M. Polivka, "Horizontal five-arm folded dipole over metal screening plane for UHF RFID of dielectric objects," *Microw. Opt. Technol. Lett.*, vol. 52, no. 10, pp. 2291-2294, Oct. 2010.

[9] C. Cho, H. Choo and I. Park, "Design of UHF small passive tag antennas," In *Proc. IEEE Antennas Propagat. Soc. Int. Symp.*, Washington DC, NY, USA, vol. 2B, pp. 349–352, 2005.

[10] H. W. Son and C. S. Pyo, "Design of RFID tag antennas using an inductively coupled feed," *Electronics Lett.*, vol. 41, no. 18, 1st Sept. 2005.

[11] S.-H. Lim, Y.-Ch. Oh, H. Lim, Y.-S. Lee and N.-H. Myung, "Analysis and design of UHF RFID tag antenna with a split ring resonator," In *Proc. IWAT 2008*, Chiba, Japan, pp. 446 – 449, 2008.

[12] Y-J. Kim and H-M. Lee, "Electrically small square loop antenna with a capacitive split ring resonator cover structure," *Microw. Opt. Technol. Lett.*, vol. 51, no. 1, pp. 831-835, March 2009.

[13] Z. Duan, S. Qu and Y. Hou, "Electrically small antenna inspired by spired split ring resonator", *Progress Electromag. Research Lett.*, vol. 7, pp. 47–57, 2009.

[14] O. S. Kim and O. Breinbjerg, "Miniaturized self-resonant split-ring resonator antenna," *Electronics Lett.*, vol. 45, no. 4, pp. 196-197, Feb. 2009.

[15] A. Holub and M. Polivka, "Electrically small loop surrounded by a "shell" of concentric split rings: Principle and properties," in *Proc. COMITE*, Prague, Czech Rep., pp. 27-30, Apr. 2010.

[16] M. Polivka and A. Holub, "Electrically small loop antenna surrounded by a "shell" of concentric split loops," in *Proc. EuCAP*, Barcelona, Spain, Apr. 2010.

[17] H. A. Wheeler, "The Radiansphere around a small antenna," *Proc. IRE*, vol. 47, no. 8, pp. 1325-1331, Aug. 1959.